

Everybody Sign Now: Translating Spoken Language to Photo Realistic Sign Language Video

Ben Saunders, Necati Cihan Camgoz, Richard Bowden
University of Surrey

{b., n.camgoz, r.bowden}@surrey.ac.uk

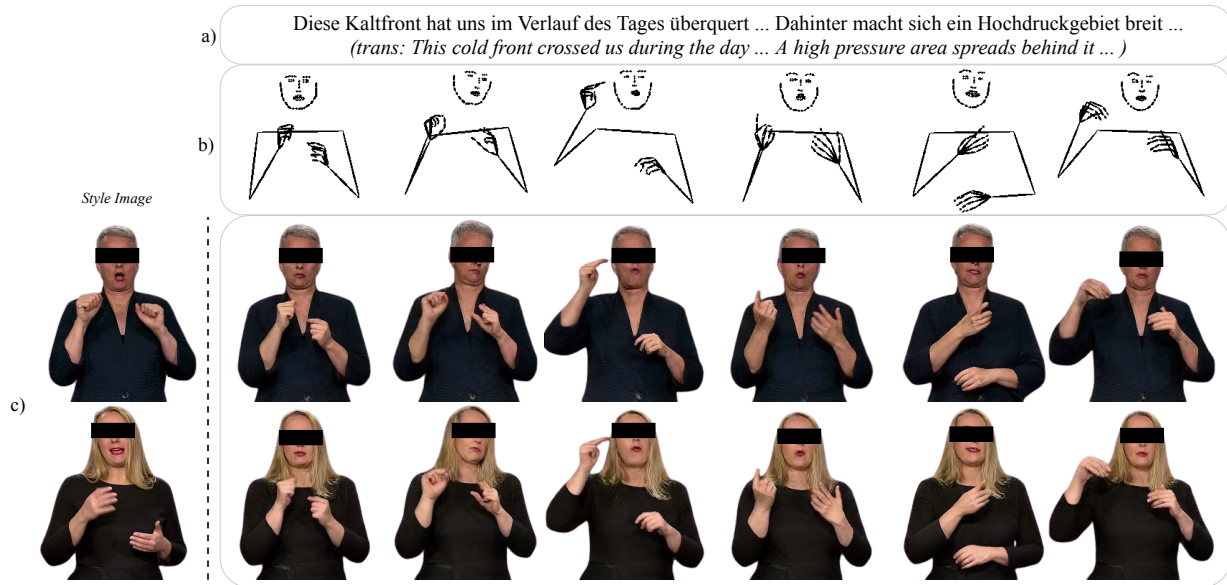


Figure 1: **Photo-Realistic Sign Language Production:** Given a spoken language sentence (a), SIGNGAN first produces a skeleton pose sequence (b) and, given a style image, generates a photo-realistic sign language video in the same style (c).

Abstract

To be truly understandable and accepted by Deaf communities, an automatic Sign Language Production (SLP) system must generate a photo-realistic signer. Prior approaches based on graphical avatars have proven unpopular, whereas recent neural SLP works that produce skeleton pose sequences have been shown to be not understandable to Deaf viewers.

In this paper, we propose SIGNGAN, the first SLP model to produce photo-realistic continuous sign language videos directly from spoken language. We employ a transformer architecture with a Mixture Density Network (MDN) formulation to handle the translation from spoken language to skeletal pose. A pose-conditioned human synthesis model is then introduced to generate a photo-realistic sign language video from the skeletal pose sequence. This allows the photo-realistic production of sign videos directly trans-

lated from written text.

We further propose a novel keypoint-based loss function, which significantly improves the quality of synthesized hand images, operating in the keypoint space to avoid issues caused by motion blur. In addition, we introduce a method for controllable video generation, enabling training on large, diverse sign language datasets and providing the ability to control the signer appearance at inference.

Using a dataset of eight different sign language interpreters extracted from broadcast footage, we show that SIGNGAN significantly outperforms all baseline methods for quantitative metrics and human perceptual studies.

1. Introduction

Sign languages are rich visual languages requiring intricate movements of both manual (hands and body) and non-manual (facial) features [42]. Sign Language Produc-

tion (SLP), the translation from spoken language sentences to sign language sequences, must replicate these intricate movements to be truly understandable by Deaf communities. Prior deep-learning approaches to SLP have mainly produced skeleton pose sequences [37, 38, 64], whereas Deaf viewers have been shown to prefer synthesized sign language videos [50].

Even though the field of pose-conditioned human synthesis has progressed significantly [2, 9, 53, 60], the application of techniques such as *Everybody Dance Now* [9] perform poorly in the SLP task [50]. Specifically, generated hands are of low quality, leading to a sign language production that is not understandable by the Deaf.

In this paper, we propose SIGNGAN, the first SLP model to produce photo-realistic continuous sign language videos directly from spoken language. Firstly, we translate from spoken language sentences to continuous skeleton pose sequences using a transformer architecture. Due to the multi-modal nature of sign languages, we use a Mixture Density Network (MDN) formulation that produces realistic and expressive sign sequences (Left of Figure 2).

The skeleton pose sequences are subsequently used to condition a video-to-video synthesis model capable of generating photo-realistic sign language videos (Right of Figure 2). Our network is the first to jointly solve the challenging tasks of continuous sign language translation and photo-realistic generation in a single neural pipeline.

Due to the high presence of motion blur in sign language datasets [15], a classical application of a discriminator over the hands could potentially lead to an increase in blurred hand generation. To avoid this, we propose a novel keypoint-based loss that uses a set of *good* hand samples to significantly improve the quality of hand image synthesis in our photo-realistic signer generation module.

To enable training on diverse sign language datasets and to make full use of the variability in appearance across signers, we propose a method for controllable video generation. This allows SIGNGAN to model a multi-modal distribution of sign language videos in different styles, as shown in Figure 1, which has been highlighted as important by Deaf focus groups [23]. In addition to providing a choice to the user about the signer’s appearance, this approach provides improved definition of the hands and face (as discussed later).

We evaluate on the challenging RWTH-PHOENIX-Weather-2014T (PHOENIX14T) corpus for continuous SLP, achieving state-of-the-art back translation results. Furthermore, we collect a dataset of sign language interpreters from broadcast footage, for photo-realistic generation. We compare against state-of-the-art pose-conditioned synthesis methods [9, 44, 54, 55] and show that SIGNGAN outperforms these approaches in the signer generation task, for quantitative evaluation and human perception studies.

The rest of this paper is organised as follows: In Sec-

tion 2, we review the previous literature in SLP and human synthesis. In Section 3, we outline the proposed SIGNGAN network. Section 4 presents quantitative and qualitative model comparison, whilst Section 5 concludes.

2. Related Work

Sign Language Production Sign language has been a focus of computer vision researchers for over 30 years [3, 41, 45]. However, research has primarily focused on initially isolated sign recognition [1, 18, 33], increasingly Continuous Sign Language Recognition (CSLR) [5, 12, 26, 25] and, only recently, the task of Sign Language Translation (SLT) [6, 7, 10, 24, 32, 61].

Sign Language Production (SLP), the translation from spoken to sign language, has been historically tackled using animated avatars [11, 22, 31]. However, there has been an increase in deep learning approaches to SLP [37, 38, 43, 59, 64]. Initial attempts have focused on the production of concatenated isolated signs that disregard the grammatical syntax of sign language [44, 64]. Saunders *et al.* proposed the first SLP model to produce continuous sign language sequences direct from source spoken language [38]. A *Progressive Transformer* model was introduced that uses a counter decoding technique to predict continuous sequences of varying length. We expand this model with a MDN formulation for more expressive sign production.

However, these works represent sign language as skeleton pose sequences, which have been shown to reduce the Deaf comprehension compared to a photo-realistic production [50]. Stoll *et al.* produced photo-realistic signers, but using low-resolution, isolated signs that do not generalise to the continuous domain [44]. In this work, we produce high-resolution photo-realistic continuous sign language videos directly from spoken language input. To improve the quality of production, we further enhance hand synthesis and introduce the ability to generate multiple signer appearances.

Pose-Conditioned Human Synthesis Generative Adversarial Networks (GANs) [17] have achieved impressive results in image [20, 34, 55, 66] and, more recently, video generation tasks [30, 49, 51, 53, 54]. Specific to pose-conditioned human synthesis, there has been concurrent research focusing on the generation of whole body [2, 29, 39, 47, 67], face [13, 27, 62, 63] and hand [28, 48, 58] images.

However, there has been no research into accurate hand generation in the context of full body synthesis, with current methods failing to generate high-quality hand images [50]. Due to the hands being high fidelity items, they are often overlooked in model optimisation. In addition, most prior work has been conditioned on poses that do not contain detailed hand poses, leading to the generation of blurry hand images [2, 54]. Chan *et al.* introduced FaceGAN for high resolution face generation [9], but no similar work has

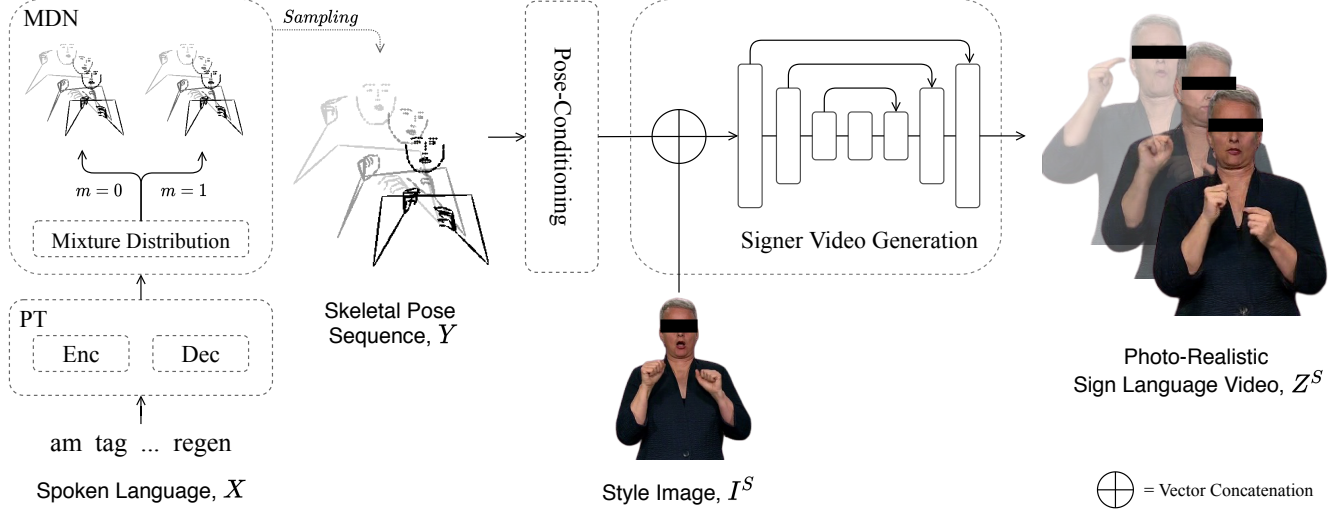


Figure 2: SIGNGAN network overview, showing the multi-stage generation of a photo-realistic sign language video, Z^S , given a spoken language sentence, X , and style image, I^S . (PT: Progressive Transformer, MDN: Mixture Density Network)

been proposed for the more challenging task of hand synthesis. However, simply adding a GAN loss on the hands serves no purpose if the original data is also blurred. In this work, we propose a keypoint-based loss using a set of *good* hand samples to enhance hand synthesis.

The task of human motion transfer, transferring motion from source to target videos via keypoint extraction, is relevant to our task [9, 57, 65]. However, there has been limited prior research into the generation of novel poses not seen in source videos or conditioned on a given input. Previous work has been restricted to conditioning pose generation on a given action [60] or audio [14, 35]. Our model first generates a sequence of unseen sign language poses given a spoken language sentence, which are subsequently used to condition our human synthesis module.

The ability to generate multiple styles at inference by separately controlling appearance and content is an important aspect of realistic human synthesis. Recent works have used dynamic weights to produce unseen appearances in a few-shot manner [53, 63], but continue to produce only a single style at inference. A semantic consistency loss for example-driven generation [52] has also been proposed, but this approach requires a manual labelling of style-consistency in the dataset and increases network computation. In this work, we introduce a novel method for controllable video generation, to enable training on large, diverse sign language datasets and support the synthesis of multiple styles from a single model.

3. Methodology

Given a source spoken language sentence, $X = (x_1, \dots, x_U)$ with U words, and a style image, I^S ,

our goal is to produce a photo-realistic sign language translation video in the same style; $Z^S = (z_1^S, \dots, z_T^S)$ with T time steps. We approach this problem as a multi-stage sequence-to-sequence task and propose the SIGNGAN network. Firstly, the spoken language sentence is translated to a sequence of sign language poses, $Y = (y_1, \dots, y_T)$, as an intermediate representation. Next, given Y and I^S , our video-to-video signer generation module generates a photo-realistic sign language video, Z^S . Figure 2 provides an overview of our network. In the remainder of this section we describe each component of SIGNGAN in detail.

3.1. Continuous Sign Language Production

To produce continuous sign language sequences from spoken language sentences, we expand the *Progressive Transformer* model proposed by Saunders *et al.* [38]. To overcome the issues of under-articulation seen in previous works [37, 38], we use a Mixture Density Network (MDN) [4] to model the variation found in sign language, as seen on the left of Figure 2. Multiple distributions are used to parameterise the entire prediction subspace, with each mixture component modelling a separate valid movement into the future. Formally, given a source sequence, $x_{1:U}$, we can model the conditional probability of producing a sign pose, y_t , as:

$$p(y_t|x_{1:U}) = \sum_{i=1}^M \alpha_i(x_{1:U}) \phi_i(y_t|x_{1:U}) \quad (1)$$

where M is the number of mixture components in the MDN. $\alpha_i(x_{1:U})$ is the mixture weight of the i^{th} distribution, regarded as a prior probability of the sign pose being generated from this mixture component. $\phi_i(y_t|x_{1:U})$ is

the conditional density of the sign pose for the i^{th} mixture, which can be expressed as a Gaussian distribution:

$$\phi_i(y_t|x_{1:U}) = \frac{1}{\sigma_i(x_{1:U})\sqrt{2\pi}} \exp\left(-\frac{\|y_t - \mu_i(x_{1:U})\|^2}{2\sigma_i(x_{1:U})^2}\right) \quad (2)$$

where $\mu_i(x_{1:U})$ and $\sigma_i(x_{1:U})$ denote the mean and variance of the i^{th} distribution. During training, we minimise the negative log likelihood of the ground truth data coming from our predicted mixture distribution. At inference, the full sign pose sequence, $Y = y_{1:T}$, can be sampled from the mixture distribution in an auto-regressive manner.

To condition our signer generation model, we convert the sign pose sequence into a heat-map representation using a pose-conditioning layer. Specifically, each limb is plotted on a separate feature channel, where a limb is defined as the connecting line between two corresponding joints. This results in a sequence of pose-conditioned features that each represents a video frame.

3.2. Photo-Realistic Sign Language Generation

To generate a photo-realistic sign language video, Z , conditioned on the produced sign language pose sequence, Y , we propose a method for video-to-video signer generation. Taking inspiration from [9], in the conditional GAN setup, a generator network, G , competes in a min-max game against a multi-scale discriminator, $D = (D_1, D_2, D_3)$. The goal of G is to synthesise images of similar quality to ground-truth images, in order to fool D . Conversely, the aim of D is to discern the “fake” images from the “real” images. For our purposes, G synthesises images of a signer given a human pose, y_t , and a style image, I^S , as shown on the right of Figure 2.

Following [20], we introduce skip connections to the architecture of G in a U -Net structure [36]. Skip connections propagate pose information across the networks, enabling the generation of fine-grained details. Specifically, we add skip connections between each down-sampling layer i and up-sampling layer $n - i$, where n is the total number of up-sampling layers.

3.2.1 Controllable Video Generation

To enable training on diverse sign language datasets, we propose a style-controllable video generation approach. A style image, I^S , is provided to condition synthesis alongside the pose sequence, (y_0, \dots, y_t) , as seen in Figure 2. During training, the model learns to associate the given style, S , with the person-specific aspects of the corresponding target image, z_t^S , such as the clothing or face. The hand pose information is signer invariant and is thus learnt independently from the style, enhancing the quality of the hand synthesis. In Section 4.2 we show the effect of training on

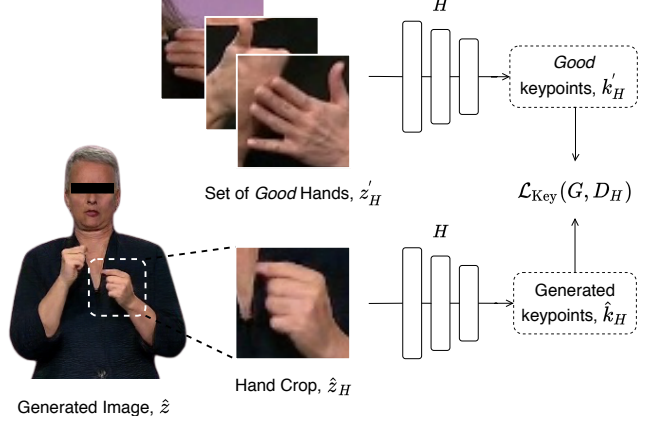


Figure 3: Hand keypoint loss overview. A keypoint discriminator, D_H , compares keypoints extracted from generated hands, \hat{k}_H and sampled good hands, k'_H .

a larger, multi-signer dataset compared to a smaller single signer corpus.

Controllable generation enables SIGNGAN to make use of the variability in signer appearance in the data. A multi-modal distribution of sign language videos in different styles, Z^S , can be produced, where $S \in \{0, N_S\}$ represents the styles seen during training. Furthermore, given a few examples of an unseen signer appearance, our model can be fine-tuned to generate a new style not seen at training, with a consistent synthesis of appearance-invariant aspects such as hands. The proposed controllable generation enables diversity in signer generation, which has been highlighted as important by Deaf focus groups [23]. Figure 4 provides examples of varying signer appearance generation.

3.2.2 Hand Keypoint Loss

Previous pose-conditioned human synthesis methods have failed to generate realistic and accurate hand images. To enhance the quality of hand synthesis, we introduce a novel loss that operates in the keypoint space, as shown in Figure 3. A pre-trained 2D hand pose estimator [16], H , is used to extract hand keypoints, k_H , from cropped hand regions (*i.e.* a 60x60 patch centered around the middle knuckle), z_H , as $k_H = H(z_H)$. We avoid operating in the image space due to the existence of blurry hand images in the dataset, whereas the extracted keypoints are invariant to motion-blur. A hand keypoint discriminator, D_H , then attempts to discern between the “real” keypoints, $k_H^* = H(z_H)$, and the “fake” keypoints, $\hat{k}_H = H(G(y_H))$, leading to the objective:

$$\begin{aligned} \mathcal{L}_{\text{KEY}}(G, D_H) = & \mathbb{E}_{y_H, z_H} [\log D_H(k_H^*)] \\ & + \mathbb{E}_{y_H} [\log(1 - D_H(\hat{k}_H))] \end{aligned} \quad (3)$$

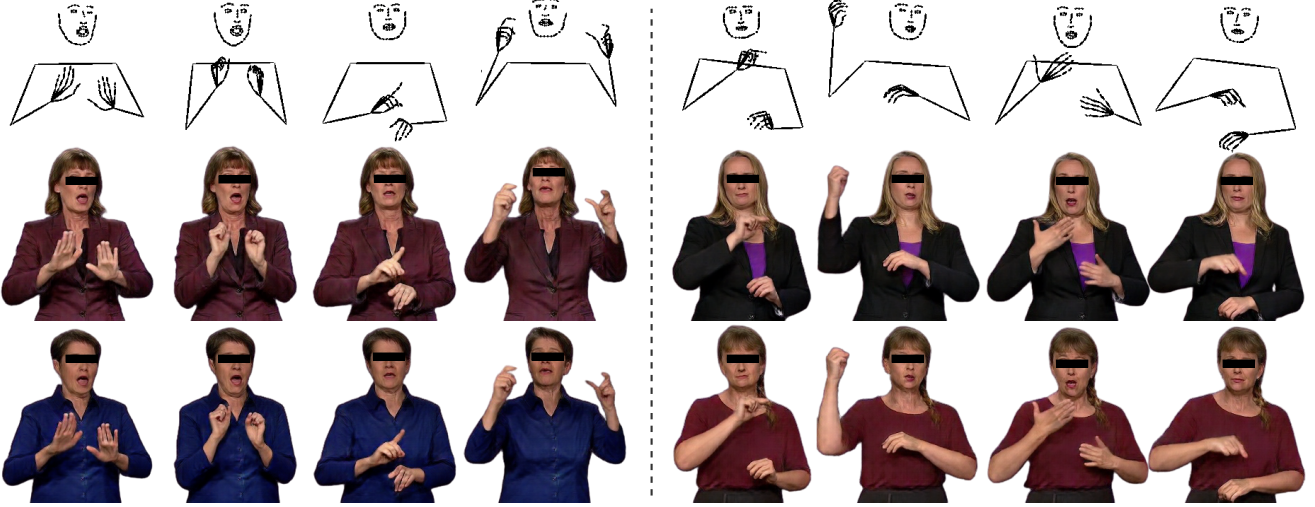


Figure 4: Photo-realistic sign language video generation examples, highlighting the variability in signer appearance.

Furthermore, we collect a set of *good* hands, z'_H , where the extracted keypoints, $k'_H = H(z'_H)$, are used to train the hand keypoint discriminator described above. This amends the objective in Equation 3 by replacing \hat{k}_H with k'_H , further enhancing the synthesis of hand images. The proposed hand keypoint loss allows the use of training samples from multiple datasets, as it is appearance invariant and removes background artifacts. Figure 4 showcases qualitative examples of our high-quality hand synthesis.

3.2.3 Full Objective

In standard image-to-image translation frameworks [20, 55], G is trained using a combination of adversarial and perceptual losses. We update the multi-scale adversarial loss, $\mathcal{L}_{GAN}(G, D)$, to reflect our controllable generation with a joint conditioning on sign pose, y_t , and style image, I^S :

$$\mathcal{L}_{GAN}(G, D) = \sum_{i=1}^k \mathbb{E}_{y_t, z_t} [\log D_i(z_t | y_t, I^S)] + \mathbb{E}_{y_t} [\log(1 - D_i(G(y_t, I^S) | y_t, I^S))] \quad (4)$$

where $k = 3$ reflects the multi-scale discriminator. The adversarial loss is supplemented with two feature-matching losses; $\mathcal{L}_{FM}(G, D)$, the discriminator feature-matching loss presented in pix2pixHD [55], and $\mathcal{L}_{VGG}(G, D)$, the perceptual reconstruction loss [21] which compares pre-trained VGGNet [40] features at multiple layers of the network. We adapt our model to the video domain with the inclusion of a temporal consistency loss, $\mathcal{L}_T(G) = (\hat{\delta} - \delta^*)^2$, where $\hat{\delta}$ and δ^* are the pixel-wise frame differences for produced and ground truth data respectively. Our full objective, \mathcal{L}_{Total} , is a weighted sum of these, alongside our proposed

hand keypoint loss (Eq. 3), as:

$$\mathcal{L}_{Total} = \min_G \left(\max_{D_i} \sum_{i=1}^k \mathcal{L}_{GAN}(G, D_i) \right) + \lambda_{FM} \sum_{i=1}^k \mathcal{L}_{FM}(G, D_i) + \lambda_{VGG} \mathcal{L}_{VGG}(G(y_t, I^S), z_t) + \lambda_{KEY} \mathcal{L}_{KEY}(G, D_H) + \lambda_T \mathcal{L}_T(G) \quad (5)$$

where $k = 3$ and λ_{FM} , λ_{VGG} , λ_{KEY} , λ_T weight the contributions of each loss.

4. Experiments

In this section, we evaluate the performance of SIGN-GAN. We first outline our experimental setup then perform quantitative, qualitative and user evaluation.

4.1. Experimental Setup

Datasets We use the challenging PHOENIX14T dataset released by Camgoz *et al.* [6] to train our continuous SLP model, with setup as proposed in Saunders *et al.* [38]. We train our human synthesis model with a collected corpus of high-quality sign language interpreter broadcast data. We use separate datasets for the two network components to overcome the limitations of each dataset. The video quality of PHOENIX14T is very low, whereas our collected interpreter data does not have aligned spoken language translations available. We apply the pose normalisation techniques of [9] to transfer between the relevant datasets.

2D upper body joints and facial landmarks are extracted using OpenPose [8]. We use a heat-map representation as pose condition, as described in Section 3.1. For the target image, we segment the sign interpreter and replace the

Approach:	DEV SET					TEST SET				
	BLEU-4	BLEU-3	BLEU-2	BLEU-1	ROUGE	BLEU-4	BLEU-3	BLEU-2	BLEU-1	ROUGE
Progressive Transformers [38]	11.82	14.80	19.97	31.41	33.18	10.51	13.54	19.04	31.36	32.46
Adversarial Training [37]	12.65	15.61	20.58	31.84	33.68	10.81	13.72	18.99	30.93	32.74
Mixture Density Networks (Ours)	11.54	14.48	19.63	30.94	33.40	11.68	14.55	19.70	31.56	33.19
SIGNGAN (Ours)	11.74	14.38	18.81	27.07	27.83	12.18	14.84	19.26	27.63	29.05

Table 1: Back translation results on the PHOENIX14T dataset for the *Text to Pose* task.

background with a consistent colour. We evaluate using an unseen sequence of a signer appearance seen during testing.

Baseline Methods We compare the performance of SIGNGAN against state-of-the-art image-to-image and video-to-video translation methods, conditioned on skeletal pose images. 1) **Everybody Dance Now (EDN)** [9] presents a method for “do as I do” motion transfer using pose as an intermediate representation. 2) **Video-to-Video Synthesis (vid2vid)** [54] uses a spatio-temporal adversarial objective to produce temporally coherent videos. 3) **Pix2PixHD** [55] is a high-definition image-to-image translation model, used to generate a video in a frame-by-frame manner. 4) **Stoll et al.** [44] apply pix2pixHD without the VGG loss to produce photo-realistic sign language videos.

Ablation Conditions We ablate our proposed model architecture with the following conditions. 1) **Skip Connections**: We start with the base condition of skip connections added to the SIGNGAN architecture. 2) **Controllable Generation**: In this condition, we include our proposed controllable video generation module. 3) **Hand Discriminator**: Here we apply a naive discriminator over the generated hand patch. 4) **Hand Keypoint Loss**: We replace the hand discriminator with our proposed hand keypoint loss. 5) **SIGNGAN (Full)**: Our final condition is the full SIGNGAN model with the addition of a hand keypoint loss compared to a set of *good* hands. Each condition is inclusive of all previous additions excluding the hand discriminator.

Evaluation Metrics We measure the quality of synthesized images using the following metrics. 1) **SSIM**: Structural Similarity [56] over the full image. 2) **Hand SSIM**: SSIM metric over a 60x60 crop of each hand. 3) **Hand Pose**: Absolute distance between 2D hand keypoints of the produced and ground truth hand images, using a pre-trained hand pose estimation model [16]. We note similar metrics were used in prior works [20, 50, 53, 54]. 4) **FID**: Fréchet Inception Distance [19] over the full image.

4.2. Quantitative Evaluation

Back Translation Our first evaluation is of our continuous SLP model. The benchmark SLP evaluation metric is back translation, which uses a pre-trained SLT model to

translate back to spoken language [38]. We use the state-of-the-art SLT [10] as our back translation model, utilizing EfficientNet-B7 [46] features as frame representations. Our models are evaluated on the *Text to Pose* task, translating directly from spoken language to sign language video.

We first evaluate our MDN formulation for the production of skeleton pose sequences, as an intermediary before photo-realistic video generation. Table 1 shows a performance increase on the test set compared to baseline methods [37, 38]. The multimodal modelling of the MDN reduces the regression to the mean found in previous deterministic models, leading to a more expressive production.

We next evaluate our full SIGNGAN model for photo-realistic sign language video generation. SIGNGAN achieves state-of-the-art back translation BLEU-4 performance on the test set, of 12.18. This highlights the increased information content available in photo-realistic videos, *i.e.* a learnt human appearance prior. In addition, this shows the importance of photo-realistic SLP for sign comprehension.

Baseline Comparisons We next evaluate our pose-conditioned signer generation by comparing performance to baselines on the same task, given a sequence of poses as input. For a fair evaluation, we first evaluate using a subset of data containing a single signer appearance. As seen in Table 2, SIGNGAN outperforms all baseline methods for all metrics, particularly for the Hand SSIM score. We believe this is due to the improved quality of synthesized hand images by using the proposed hand keypoint loss.

We next evaluate using a larger, multiple signer dataset in Table 3, to show the effect of our controllable generation module. SIGNGAN again outperforms all baseline methods and achieves a significant performance increase compared to training on a single signer corpus. We believe this is due to the larger variety of hand and body pose present

	SSIM ↑	Hand SSIM ↑	Hand Pose ↓	FID ↓
EDN [9]	0.726	0.545	22.88	29.62
vid2vid [54]	0.726	0.551	22.76	27.51
Pix2PixHD [55]	0.726	0.541	22.95	32.88
Stoll et al. [44]	0.733	0.547	22.81	73.38
SIGNGAN (Ours)	0.742	0.588	22.68	24.10

Table 2: Baseline model comparison results, on a single signer subset of the data.

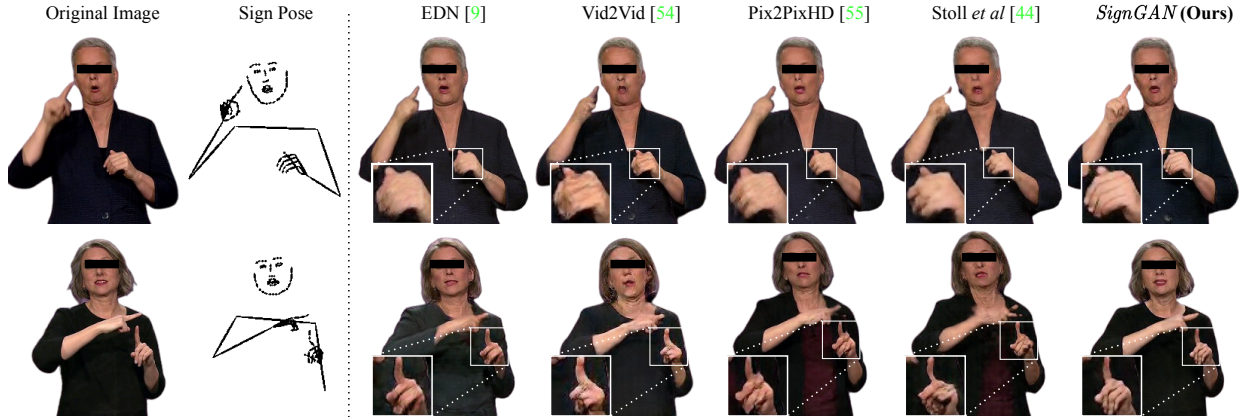


Figure 5: Baseline comparisons trained on a single signer (top) or multiple signer (bottom) dataset. Best viewed in colour.

	SSIM \uparrow	Hand SSIM \uparrow	Hand Pose \downarrow	FID \downarrow
EDN [9]	0.737	0.553	23.09	41.54
vid2vid [54]	0.750	0.570	22.51	56.17
Pix2PixHD [55]	0.737	0.553	23.06	42.57
Stoll <i>et al.</i> [44]	0.727	0.533	23.17	64.01
SIGNGAN (Ours)	0.759	0.605	22.05	27.75

Table 3: Baseline model comparison results, on the full dataset containing multiple signers.

in the diverse dataset, as well as the presence of multiple signers acting as a regularizer. Conversely, baseline methods perform significantly worse for FID scores, due to the lack of ability to control the signer appearance.

Ablation Study We perform an ablation study of SIGNGAN using the multiple signer dataset, with results in Table 4. Our skip connection architecture achieves a strong performance, with SSIM and hand SSIM higher than all baseline models bar vid2vid. The importance of our controllable generation is highlighted by an improvement in SSIM and FID scores when applied. Without this, a generated video will be temporally inconsistent with a blurred appearance.

The hand discriminator performs poorly for both SSIM and hand SSIM, due to the generation of blurred hands. However, our proposed hand keypoint loss improves performance, particularly for hand SSIM, emphasizing the importance of an adversarial loss invariant to blurring. Finally, the full SIGNGAN model performs best, particularly for the hand SSIM score. We believe this is due to the increased quality of images used to train our hand keypoint discriminator, prompting an enhanced synthesis.

Perceptual Study We perform a perceptual study of our video generation, showing participants pairs of 10 second videos generated by SIGNGAN and a corresponding base-

	SSIM \uparrow	Hand SSIM \uparrow	Hand Pose \downarrow	FID \downarrow
Skip Connections	0.743	0.582	22.87	39.33
Controllable Gen.	0.752	0.587	22.09	32.22
Hand Discriminator	0.738	0.565	22.81	39.22
Hand Keypoint Loss	0.758	0.598	21.89	29.02
SIGNGAN (Full)	0.759	0.605	22.05	27.75

Table 4: Ablation study results, on a multiple signer dataset.

line method. We generated videos using either a single or multiple signer dataset. Participants were asked to select which video was more visually realistic, with a separate focus on the body and hands. In total, 46 participant completed the study, of which 28% were signers, each viewing 2 randomly selected videos from each of the baselines. Table 5 shows the percentage of participants who preferred the outputs of SIGNGAN to the baseline method.

It can be clearly seen that our outputs were preferred by participants compared to all baseline models for both body (97.3% average) and hand (96.5% average) synthesis. Vid2vid was the strongest contender, with our productions preferred only 91% of the time, compared to 99.7% for Stoll *et al.* In addition, SIGNGAN was preferred when the models were trained on the multiple signer dataset, highlighting the effect of our controllable video generation module.

	Single Signer		Multiple Signer	
	Body	Hand	Body	Hand
EDN [9]	97.8%	97.8%	100%	97.8%
vid2vid [54]	97.8%	95.6%	85.9%	84.8%
Pix2PixHD [55]	96.7%	96.7%	98.9%	100%
Stoll <i>et al.</i> [44]	98.9%	100%	100%	100%

Table 5: Perceptual study results, showing the percentage of participants who preferred **our** method to the baseline trained on a single or multiple signer dataset.

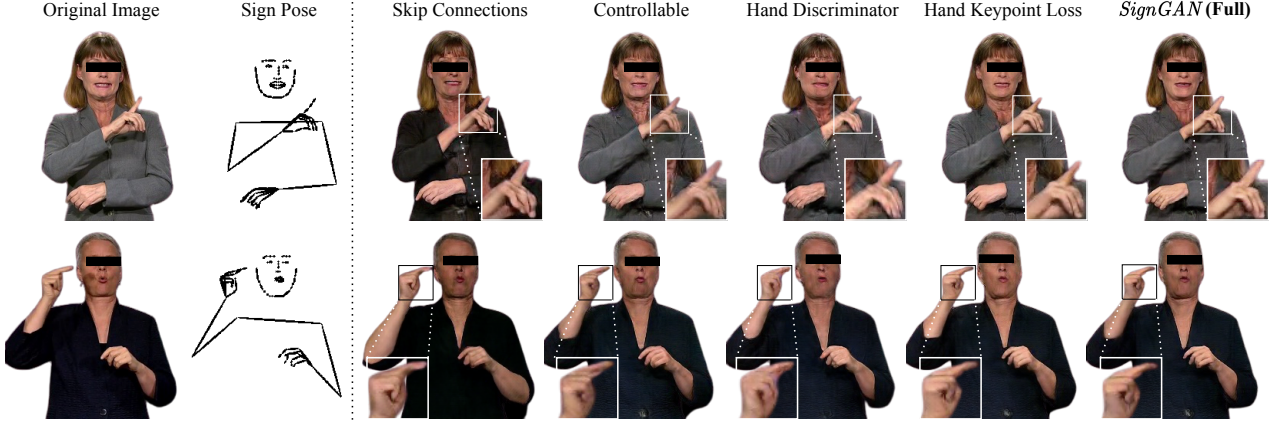


Figure 6: Ablation Study of SIGNGAN trained on the multiple signer dataset. Best viewed in colour.

4.3. Qualitative Evaluation

Baseline Comparison As seen in the baseline comparisons of Figure 5, SIGNGAN clearly generates the most natural-looking hands. Other approaches generate hands that are blurred, due to the existence of motion blur in the training data and the lack of a hand-specific loss. When trained on the larger, multiple signer dataset (bottom), baselines struggle to generate a consistent signer appearance. In contrast, SIGNGAN generates an identical style to the original image, due to the proposed controllable video generation. Although superior results can be seen in image synthesis, we believe more significant differences can be seen in the video outputs. We recommend the reader to view the comparison videos provided in supplementary material.

Ablation Study Figure 6 shows qualitative results when ablating our model. The effect of the proposed controllable video generation is highlighted, as without it the signer appearance is inconsistent. The classic hand discriminator can be seen to produce blurry hands due to the existence of motion blur in the training dataset. Our proposed hand keypoint loss generates higher quality hands with considerable detail and sharper synthesis, particularly when trained using a set of *good* hands in the SIGNGAN (full) setup. Although the effect is subtle, this is an important addition for the understanding of sign language videos, where the focus is often on the manual features. Figure 7 showcases the full repertoire of interpreters generated from a single model, showing the control available to the viewer.

5. Conclusion

Sign Language Production (SLP) requires the generation of photo-realistic sign language videos to be understandable by the Deaf [50], whereas prior work has produced skeletal pose sequences. In this paper, we proposed SIGNGAN,

the first SLP model to produce photo-realistic continuous sign language videos directly from spoken language. We employed a transformer architecture with a Mixture Density Network (MDN) formulation to translate from spoken language to skeletal pose. Pose sequences are subsequently used to condition the generation of a photo-realistic sign language video using a human synthesis module.

We proposed a novel keypoint-based loss function to significantly improve the quality of hand synthesis, operating in the keypoint space to avoid issues caused by motion blur. Additionally, we proposed a method for controllable video generation, enabling training on large, diverse sign language datasets and providing the ability to control the signer appearance at inference. Finally, we collected a varied dataset of sign language interpreters and showed that SIGNGAN outperforms all baseline methods for quantitative evaluation and human perceptual studies.



Figure 7: Variable generation of 8 signer appearances.

6. Acknowledgements

This work received funding from the SNSF Sinergia project 'SMILE' (CRSII2 160811), the European Union's Horizon2020 research and innovation programme under grant agreement no. 762021 'Content4All' and the EPSRC project 'ExTOL' (EP/R03298X/1). This work reflects only the authors view and the Commission is not responsible for any use that may be made of the information it contains. We would also like to thank NVIDIA Corporation for their GPU grant. We would like to thank SWISSTXT for access to the broadcast footage.

References

- [1] Epameinondas Antonakos, Vassilis Pitsikalis, Isidoros Rodomagoulakis, and Petros Maragos. Unsupervised Classification of Extreme Facial Events using Active Appearance Models Tracking for Sign Language Videos. In *19th IEEE International Conference on Image Processing (ICIP)*, 2012. 2
- [2] Guha Balakrishnan, Amy Zhao, Adrian V Dalca, Fredo Durand, and John Guttag. Synthesizing Images of Humans in Unseen Poses. In *Proceedings of the IEEE Conference on Computer Vision and Pattern Recognition (CVPR)*, 2018. 2
- [3] Britta Bauer, Hermann Hienz, and K-F Kraiss. Video-Based Continuous Sign Language Recognition using Statistical Methods. In *Proceedings of International Conference on Pattern Recognition (ICPR)*, 2000. 2
- [4] Christopher M Bishop. Mixture Density Networks. *Technical Report, Citeseer*, 1994. 3
- [5] Necati Cihan Camgoz, Simon Hadfield, Oscar Koller, and Richard Bowden. SubUNets: End-to-end Hand Shape and Continuous Sign Language Recognition. In *Proceedings of the IEEE International Conference on Computer Vision (ICCV)*, 2017. 2
- [6] Necati Cihan Camgoz, Simon Hadfield, Oscar Koller, Hermann Ney, and Richard Bowden. Neural Sign Language Translation. In *Proceedings of the IEEE Conference on Computer Vision and Pattern Recognition (CVPR)*, 2018. 2, 5
- [7] Necati Cihan Camgoz, Oscar Koller, Simon Hadfield, and Richard Bowden. Multi-channel Transformers for Multi-articulatory Sign Language Translation. In *Assistive Computer Vision and Robotics Workshop (ACVR)*, 2020. 2
- [8] Zhe Cao, Gines Hidalgo, Tomas Simon, Shih-En Wei, and Yaser Sheikh. OpenPose: Realtime Multi-Person 2D Pose Estimation using Part Affinity Fields. In *Proceedings of the IEEE Conference on Computer Vision and Pattern Recognition (CVPR)*, 2017. 5
- [9] Caroline Chan, Shiry Ginosar, Tinghui Zhou, and Alexei A Efros. Everybody Dance Now. In *Proceedings of the IEEE International Conference on Computer Vision (CVPR)*, 2019. 2, 3, 4, 5, 6, 7
- [10] Necati Cihan Camgoz, Oscar Koller, Simon Hadfield, and Richard Bowden. Sign Language Transformers: Joint End-to-end Sign Language Recognition and Translation. In *Proceedings of the IEEE Conference on Computer Vision and Pattern Recognition (CVPR)*, 2020. 2, 6
- [11] Stephen Cox, Michael Lincoln, Judy Tryggvason, Melanie Nakisa, Mark Wells, Marcus Tutt, and Sanja Abbott. TESSA, a System to Aid Communication with Deaf People. In *Proceedings of the ACM International Conference on Assistive Technologies*, 2002. 2
- [12] Runpeng Cui, Hu Liu, and Changshui Zhang. Recurrent Convolutional Neural Networks for Continuous Sign Language Recognition by Staged Optimization. In *Proceedings of the IEEE Conference on Computer Vision and Pattern Recognition (CVPR)*, 2017. 2
- [13] Yu Deng, Jiaolong Yang, Dong Chen, Fang Wen, and Xin Tong. Disentangled and Controllable Face Image Generation via 3D Imitative-Contrastive Learning. In *Proceedings of the IEEE Conference on Computer Vision and Pattern Recognition (CVPR)*, 2020. 2
- [14] João P Ferreira, Thiago M Coutinho, Thiago L Gomes, José F Neto, Rafael Azevedo, Renato Martins, and Erickson R Nascimento. Learning to Dance: A Graph Convolutional Adversarial Network to Generate Realistic Dance Motions from Audio. *Computers & Graphics*, 2020. 3
- [15] Jens Forster, Christoph Schmidt, Oscar Koller, Martin Bellgardt, and Hermann Ney. Extensions of the Sign Language Recognition and Translation Corpus RWTH-PHOENIX-Weather. In *Proceedings of the International Conference on Language Resources and Evaluation (LREC)*, 2014. 2
- [16] Lihao Ge, Zhou Ren, Yuncheng Li, Zehao Xue, Yingying Wang, Jianfei Cai, and Junsong Yuan. 3D Hand Shape and Pose Estimation from a Single RGB Image. In *Proceedings of the IEEE Conference on Computer Vision and Pattern Recognition (CVPR)*, 2019. 4, 6
- [17] Ian Goodfellow, Jean Pouget-Abadie, Mehdi Mirza, Bing Xu, David Warde-Farley, Sherjil Ozair, Aaron Courville, and Yoshua Bengio. Generative Adversarial Nets. In *Proceedings of the Advances in Neural Information Processing Systems (NIPS)*, 2014. 2
- [18] Kirsti Grobel and Marcell Assan. Isolated Sign Language Recognition using Hidden Markov Models. In *IEEE International Conference on Systems, Man, and Cybernetics*, 1997. 2
- [19] Martin Heusel, Hubert Ramsauer, Thomas Unterthiner, Bernhard Nessler, and Sepp Hochreiter. GANs Trained by a Two Time-Scale Update Rule Converge to a Local Nash Equilibrium. In *Proceedings of the Advances in Neural Information Processing Systems (NIPS)*, 2017. 6
- [20] Phillip Isola, Jun-Yan Zhu, Tinghui Zhou, and Alexei A Efros. Image-to-Image Translation with Conditional Adversarial Networks. In *Proceedings of the IEEE Conference on Computer Vision and Pattern Recognition (CVPR)*, 2017. 2, 4, 5, 6
- [21] Justin Johnson, Alexandre Alahi, and Li Fei-Fei. Perceptual Losses for Real-Time Style Transfer and Super-Resolution. In *Proceedings of the European Conference on Computer Vision (ECCV)*, 2016. 5
- [22] Kostas Karpouzis, George Caridakis, S-E Fotinea, and Eleni Efthimiou. Educational Resources and Implementation of a Greek Sign Language Synthesis Architecture. *Computers & Education (CAEO)*, 2007. 2

- [23] Michael Kipp, Quan Nguyen, Alexis Heloir, and Silke Matthes. Assessing the Deaf User Perspective on Sign Language Avatars. In *The Proceedings of the 13th International ACM SIGACCESS Conference on Computers and Accessibility (ASSETS)*, 2011. 2, 4
- [24] Sang-Ki Ko, Chang Jo Kim, Hyedong Jung, and Choongsang Cho. Neural Sign Language Translation based on Human Keypoint Estimation. *Applied Sciences*, 2019. 2
- [25] Oscar Koller, Necati Cihan Camgoz, Richard Bowden, and Hermann Ney. Weakly Supervised Learning with Multi-Stream CNN-LSTM-HMMs to Discover Sequential Parallelism in Sign Language Videos. *IEEE Transactions on Pattern Analysis and Machine Intelligence (TPAMI)*, 2019. 2
- [26] Oscar Koller, Jens Forster, and Hermann Ney. Continuous Sign Language Recognition: Towards Large Vocabulary Statistical Recognition Systems Handling Multiple Signers. *Computer Vision and Image Understanding (CVIU)*, 2015. 2
- [27] Marek Kowalski, Stephan J Garbin, Virginia Estellers, Tadas Baltrušaitis, Matthew Johnson, and Jamie Shotton. CONFIG: Controllable Neural Face Image Generation. In *Proceedings of the European Conference on Computer Vision (ECCV)*, 2020. 2
- [28] Yahui Liu, Marco De Nadai, Gloria Zen, Nicu Sebe, and Bruno Lepri. Gesture-to-Gesture Translation in the Wild via Category-Independent Conditional Maps. In *Proceedings of the 27th ACM International Conference on Multimedia*, 2019. 2
- [29] Liqian Ma, Xu Jia, Qianru Sun, Bernt Schiele, Tinne Tuytelaars, and Luc Van Gool. Pose Guided Person Image Generation. In *Advances in Neural Information Processing Systems (NIPS)*, 2017. 2
- [30] Arun Mallya, Ting-Chun Wang, Karan Sapra, and Ming-Yu Liu. World-Consistent Video-to-Video Synthesis. In *Proceedings of the European Conference on Computer Vision (ECCV)*, 2020. 2
- [31] John McDonald, Rosalee Wolfe, Jerry Schnepf, Julie Hochgesang, Diana Gorman Jamrozik, Marie Stumbo, Larian Berke, Melissa Bialek, and Farah Thomas. Automated Technique for Real-Time Production of Lifelike Animations of American Sign Language. *Universal Access in the Information Society (UAIS)*, 2016. 2
- [32] Alptekin Orbay and Lale Akarun. Neural Sign Language Translation by Learning Tokenization. In *IEEE International Conference on Automatic Face and Gesture Recognition (FG)*, 2020. 2
- [33] Oğulcan Özdemir, Necati Cihan Camgöz, and Lale Akarun. Isolated Sign Language Recognition using Improved Dense Trajectories. In *Proceedings of the Signal Processing and Communication Application Conference (SIU)*, 2016. 2
- [34] Alec Radford, Luke Metz, and Soumith Chintala. Unsupervised Representation Learning with Deep Convolutional Generative Adversarial Networks. *arXiv preprint arXiv:1511.06434*, 2015. 2
- [35] Xuanchi Ren, Haoran Li, Zijian Huang, and Qifeng Chen. Self-Supervised Dance Video Synthesis Conditioned on Music. In *Proceedings of the 28th ACM International Conference on Multimedia*, 2020. 3
- [36] Olaf Ronneberger, Philipp Fischer, and Thomas Brox. U-net: Convolutional Networks for Biomedical Image Segmentation. In *International Conference on Medical Image Computing and Computer-Assisted Intervention (MIC-CAI)*, 2015. 4
- [37] Ben Saunders, Necati Cihan Camgoz, and Richard Bowden. Adversarial Training for Multi-Channel Sign Language Production. In *Proceedings of the British Machine Vision Conference (BMVC)*, 2020. 2, 3, 6
- [38] Ben Saunders, Necati Cihan Camgoz, and Richard Bowden. Progressive Transformers for End-to-End Sign Language Production. In *Proceedings of the European Conference on Computer Vision (ECCV)*, 2020. 2, 3, 5, 6
- [39] Aliaksandr Siarohin, Enver Sangineto, Stéphane Lathuilière, and Nicu Sebe. Deformable GANs for Pose-Based Human Image Generation. In *Proceedings of the IEEE Conference on Computer Vision and Pattern Recognition (CVPR)*, 2018. 2
- [40] Karen Simonyan and Andrew Zisserman. Very Deep Convolutional Networks for Large-Scale Image Recognition. *arXiv preprint arXiv:1409.1556*, 2014. 5
- [41] Thad Starner and Alex Pentland. Real-time American Sign Language Recognition from Video using Hidden Markov Models. *Motion-Based Recognition*, 1997. 2
- [42] William C Stokoe. Sign Language Structure. *Annual Review of Anthropology*, 1980. 1
- [43] Stephanie Stoll, Necati Cihan Camgoz, Simon Hadfield, and Richard Bowden. Sign Language Production using Neural Machine Translation and Generative Adversarial Networks. In *Proceedings of the British Machine Vision Conference (BMVC)*, 2018. 2
- [44] Stephanie Stoll, Necati Cihan Camgoz, Simon Hadfield, and Richard Bowden. Text2Sign: Towards Sign Language Production using Neural Machine Translation and Generative Adversarial Networks. *International Journal of Computer Vision (IJCV)*, 2020. 2, 6, 7
- [45] Shinichi Tamura and Shingo Kawasaki. Recognition of Sign Language Motion Images. *Pattern Recognition*, 1988. 2
- [46] Mingxing Tan and Quoc Le. EfficientNet: Rethinking Model Scaling for Convolutional Neural Networks. In *International Conference on Machine Learning (ICML)*, 2019. 6
- [47] Hao Tang, Song Bai, Li Zhang, Philip HS Torr, and Nicu Sebe. XingGAN for Person Image Generation. In *Proceedings of the European Conference on Computer Vision (ECCV)*, 2020. 2
- [48] Hao Tang, Wei Wang, Dan Xu, Yan Yan, and Nicu Sebe. GestureGAN for Hand Gesture-to-Gesture Translation in the wild. In *Proceedings of the 26th ACM International Conference on Multimedia*, 2018. 2
- [49] Sergey Tulyakov, Ming-Yu Liu, Xiaodong Yang, and Jan Kautz. MoCoGAN: Decomposing Motion and Content for Video Generation. In *Proceedings of the IEEE Conference on Computer Vision and Pattern Recognition (CVPR)*, 2018. 2
- [50] Lucas Ventura, Amanda Duarte, and Xavier Giró-i Nieto. Can Everybody Sign Now? Exploring Sign Language Video

- Generation from 2D Poses. In *ECCV Sign Language Recognition, Translation and Production Workshop*, 2020. 2, 6, 8
- [51] Carl Vondrick, Hamed Pirsiavash, and Antonio Torralba. Generating Videos with Scene Dynamics. In *Advances in Neural Information Processing Systems (NIPS)*, 2016. 2
- [52] Miao Wang, Guo-Ye Yang, Ruilong Li, Run-Ze Liang, Song-Hai Zhang, Peter M Hall, and Shi-Min Hu. Example-Guided Style-Consistent Image Synthesis from Semantic Labeling. In *Proceedings of the IEEE Conference on Computer Vision and Pattern Recognition (CVPR)*, 2019. 3
- [53] Ting-Chun Wang, Ming-Yu Liu, Andrew Tao, Guilin Liu, Jan Kautz, and Bryan Catanzaro. Few-shot Video-to-Video Synthesis. In *Advances in Neural Information Processing Systems (NeurIPS)*, 2019. 2, 3, 6
- [54] Ting-Chun Wang, Ming-Yu Liu, Jun-Yan Zhu, Guilin Liu, Andrew Tao, Jan Kautz, and Bryan Catanzaro. Video-to-Video Synthesis. In *Advances in Neural Information Processing Systems (NIPS)*, 2018. 2, 6, 7
- [55] Ting-Chun Wang, Ming-Yu Liu, Jun-Yan Zhu, Andrew Tao, Jan Kautz, and Bryan Catanzaro. High-Resolution Image Synthesis and Semantic Manipulation with Conditional GANs. In *Proceedings of the IEEE Conference on Computer Vision and Pattern Recognition (CVPR)*, 2018. 2, 5, 6, 7
- [56] Zhou Wang, Alan C Bovik, Hamid R Sheikh, and Eero P Simoncelli. Image Quality Assessment: From Error Visibility to Structural Similarity. *IEEE Transactions on Image Processing*, 2004. 6
- [57] Dongxu Wei, Xiaowei Xu, Haibin Shen, and Kejie Huang. GAC-GAN: A General Method for Appearance-Controllable Human Video Motion Transfer. *IEEE Transactions on Multimedia*, 2020. 3
- [58] Zhenyu Wu, Duc Hoang, Shih-Yao Lin, Yusheng Xie, Liangjian Chen, Yen-Yu Lin, Zhangyang Wang, and Wei Fan. MM-Hand: 3D-Aware Multi-Modal Guided Hand Generative Network for 3D Hand Pose Synthesis. *arXiv preprint arXiv:2010.01158*, 2020. 2
- [59] Qinkun Xiao, Minying Qin, and Yuting Yin. Skeleton-based Chinese Sign Language Recognition and Generation for Bidirectional Communication between Deaf and Hearing People. In *Neural Networks*, 2020. 2
- [60] Ceyuan Yang, Zhe Wang, Xinge Zhu, Chen Huang, Jianping Shi, and Dahua Lin. Pose Guided Human Video Generation. In *Proceedings of the European Conference on Computer Vision (ECCV)*, 2018. 2, 3
- [61] Kayo Yin. Sign Language Translation with Transformers. *arXiv preprint arXiv:2004.00588*, 2020. 2
- [62] Egor Zakharov, Aleksei Ivakhnenko, Aliaksandra Shysheya, and Victor Lempitsky. Fast bi-layer neural synthesis of one-shot realistic head avatars. In *Proceedings of the European Conference on Computer Vision (ECCV)*, 2020. 2
- [63] Egor Zakharov, Aliaksandra Shysheya, Egor Burkov, and Victor Lempitsky. Few-Shot Adversarial Learning of Realistic Neural Talking Head Models. In *Proceedings of the IEEE International Conference on Computer Vision (CVPR)*, 2019. 2, 3
- [64] Jan Zelinka and Jakub Kanis. Neural Sign Language Synthesis: Words Are Our Glosses. In *The IEEE Winter Conference on Applications of Computer Vision (WACV)*, 2020. 2
- [65] Yipin Zhou, Zhaowen Wang, Chen Fang, Trung Bui, and Tamara Berg. Dance Dance Generation: Motion Transfer for Internet Videos. In *Proceedings of the IEEE International Conference on Computer Vision Workshops*, 2019. 3
- [66] Jun-Yan Zhu, Taesung Park, Phillip Isola, and Alexei A Efros. Unpaired Image-to-Image Translation using Cycle-Consistent Adversarial Networks. In *Proceedings of the IEEE International Conference on Computer Vision (ICCV)*, 2017. 2
- [67] Zhen Zhu, Tengting Huang, Baoguang Shi, Miao Yu, Bofei Wang, and Xiang Bai. Progressive Pose Attention Transfer for Person Image Generation. In *Proceedings of the IEEE Conference on Computer Vision and Pattern Recognition (CVPR)*, 2019. 2